Published in: Colloid polymer science (2000), vol. 278, iss. 10, pp. 993-999
Status: Postprint (Author's version)

Surface structure of thin film blends of polystyrene and poly(*n*-butyl methacrylate)

S. Affrossman [(1)], R. Jerome[(2)], S. A. O'Neill[(1)], T. Schmitt[(3)], M. Stamm[(4)]

(1) Department of Pure and Applied Chemistry, University of Strathclyde Cathedral Street, Glasgow Gl 1XL, UK
(2) Centre for Education and Research on Macromolecules, University of Liège Sart-Tilman B6, 4000 Liège, Belgium
(3) Max-Planck-Institut fur Polymerforschung, Postfach 3148, 55021 Mainz Germany
(4) Institut fur Polymerforschung Dresden e. V., Hohe Strasse 6, Postfach 12 04 11 01005 Dresden, Germany

Abstract
Thin films of blends of polystyrene (PS) and poly(*n*-butyl methacrylate) (PBMA) were prepared by spin-casting onto silicon wafers in order to map the lateral distribution of the two polymers. The surfaces were examined by atomic force microscopy (AFM) secondary ion mass spectroscopy X-ray photoelectron spectroscopy (XPS) and photoemission electron microscopy (PEEM). Films with PBMA contents of 50% w/w or less were relatively smooth, but further increase in the PBMA content produced, initially, protruding PS ribbons and then, for PBMA ≥80% w/w, isolated PS islands. At all concentrations the topmost surface (0.5-1.0 nm) was covered by PBMA, whilst the PBMA concentration in the near-surface region, measured by XPS, increased with bulk content to eventual saturation. PEEM measurements of a PS-PBMA film at the composition at which ribbon features were observed by AFM also showed a PS-rich ribbon structure surrounded by a sea of mainly PBMA.

Key words : Polymer blends - Thin films - Topography - Polystyrene

Introduction

Films of partially compatible polymer blends which are only a small number of polymer molecular diameters in thickness, i.e. less than about 100 nm, can exhibit surface structures which arise from several interfacial forces acting on the polymer phases during film formation in a confined geometry [1-3]. Depending on the phase diagram of the polymer blend, i.e. the lower critical solubility temperature or the upper critical solubility temperature, it may be possible to anneal the film in the one-phase or the two-phase region, removing residual solvent and forming smooth or rough equilibrated films interchangeably [4].
Generally, the thin films are produced by spin-casting and, consequently, the structure of the initial cast film is influenced by the restrictions in polymer mobility in a ternary system where the solvent is being rapidly removed. Thus, the initial structure may contain meta-stable features because polymer diffusion is effectively frozen. The formation of topography in the initial cast films depends on the phase separation of the polymer components which, in turn, is a function of the polymer compatibility. Studies of a series of polymer blends of deuterated polystyrene and polystyrene partially substituted with bromine, dPS-PBr$_x$S ($0 \leq x \leq 1$), have established that the polymer compatibility varies monotonically with the extent of bromine substitution [5] and that topography develops in thin films of the blends when the bromine content increases, and hence when the compatibility decreases, to a certain level [6]. The other factors which influence the formation of topography during spin-casting are the polymer—substrate and polymer—air and polymer—polymer interfacial tensions, for example, topography may be altered, or removed, by modifying the substrate surface [3, 7].
Thin case films of PS-polyester blends also exhibit topography. Tanaka et al. [7] investigated the surface structure of thin films of symmetric blends of PS with poly(methyl methacrylate) (PMMA) on various substrates and showed that the PMMA blocks protrude, with the relative area of the PMMA domains increasing as the substrate became more hydrophobic. X-ray photoelectron spectroscopy (XPS) showed that the surface fraction of PMMA was always less than the bulk fraction, in accord with the higher surface energy compared to that of PS. Recently, Tanaka et al. [8] studied the surface structure of 6-700-nm thick films of blends of a high-molecular-weight PS with up to 10% w/w of various lower-molecular-weight PMMAs. Unless the molecular weight of the PMMA was very low, they observed topographical features in the form of rims of raised material at the boundary of circular

PMMA blocks. The low-molecular-weight PMMAs segregated to the polymer—air interface, which was attributed to chain-end effects overcoming the higher surface energy and, consequently, the extent of segregation decreased with an increase in M_n.

A detailed examination of the influence of the casting solvent on thin film structure by Walheim et al. [9] showed that the protruding phase of the PS-PMMA system could be reversed by suitable choice of solvent and substrate. The variations in solubility of the polymer components in the solvents and the polymer-substrate interactions were correlated with the changes in topography.

PS and PMMA form a highly incompatible blend. Increasing the length of the ester alkyl chain gives more compatibility and in this work blends of poly(*n*-butyl methacrylate) (PBMA) with PS were investigated to determine the extent to which the relationship between compatibility and topography, observed for PS-PBr_xS blends, applies to the PS-polyester system. Atomic force microscopy (AFM) and photoemission electron microscopy (PEEM) measurements provide topography and specific imaging of the lateral distribution of the PS and PBMA in the film, respectively, while XPS and secondary ion mass spectroscopy (SIMS) provide information on the surface segregation of components averaged over a relatively large area.

Experimental

Materials

A pure deuterated polymer, prepared by anionic polymerisation, was used as the PS component in the XPS, SIMS and AFM measurements. It has the advantage in the SIMS analysis of being less likely to be confused with organic impurities. Nondeuterated and deuterated PS behave similarly in blends with PBrS, the difference in polarity of the components greatly outweighing isotopic differences. The present study combines the nonpolar PS with a polar polyester; therefore, data from a related PEEM study of PS-PBMA using a nondeuterated PS were considered relevant.

PBMA was prepared at Liège by anionic polymerisation of *n*-butyl methacrylate with butyllithium as initiator in tetrahydrofuran at -78 °C. The polymer was precipitated in a water—ethanol mixture, filtered and dried in a vacuum.

Size-exclusion chromatography, to obtain molecular weights and distributions, was performed using PS standards for PS and PMMA standards for PBMA.

The following data were obtained: dPS, M_n = 157,000 g/mol, M_w/M_n = 1.09; PBMA, M_n = 124,000 g/mol, M_w/M_n = 1.10 (samples used for AFM, XPS and SIMS); PS, M_n = 134,439 g/mol, M_w/M_n = 1.037; PBMA, M_n = 84,466 g/mol, M_w/M_n = 1.03 (sample used for PEEM).

In order to analyse the XPS and SIMS data it is necessary to calculate the monomer fraction of the components from the composition percent weight per weight by dividing the component weights by the monomer molecular weights. The monomer fractions are listed in Table 1.

Film formation

Films were prepared by dropwise addition of a 1 or 2% w/w toluene solution of the polymer mixture onto silicon wafers spinning at 4000 rpm. The wafers were cleaned initially with sulphuric/peroxide solution, which leaves the native oxide on the surface. In order to preserve the initial structure the films were not annealed.

Film thickness

The film thickness of the samples examined by AFM, XPS and SIMS, determined with a Sloan Dektak lla profilometer, was 43 ± 4 nm. The thickness of the film used in the PEEM study was measured by null ellipsometry as 96 ± 2 nm.

Atomic force microscopy

The parameters for the instrument, Burleigh ARIS-3300 Personal AFM, have been described previously [3]. The microscope was operated in contact mode and no image smoothing was applied.

Photoemission electron microscopy

The PEEM measurements were carried out at the synchrotron radiation facility BESSY 1 at beamline PM 3 with an SX-700/3 monochromator. The instrument, IS-PEEM is described in detail elsewhere [10]. The photoelectron microscope comprises an electrostatic tetrode objective lens, a contrast aperture, a stigmator/ deflector for maximum resolution, an iris aperture for enhancement of contrast and resolution and two projective lenses. The lateral electron distribution emitted from the illumination of the thin polymer film with synchrotron radiation is intensified by a multichannel plate and made visible by a fluorescent screen.

Published in: Colloid polymer science (2000), vol. 278, iss. 10, pp. 993-999
Status: Postprint (Author's version)

Table 1 Blend compositions

% w/w poly(*n*-butyl methacrylate)	Monomer fraction
10	0.08
30	0.25
50	0.44
60	0.54
70	0.65
80	0.76
90	0.88

The image acquisition from the fluorescent screen was obtained with a charge-coupled-device camera and the captured images were stored in a computer for processing.
The PEEM investigation provided spectromicroscopic mapping of the lateral distribution of the two polymers in the 96-nm thick PS-PBMA film with a PBMA content of 70% w/w. This film is shown to have a similar ribbon structure to the 43-nm thick films with the same PBMA content of the series examined by AFM, XPS and SIMS. The PEEM was operated in the near-edge X-ray absorption fine structure (NEXAFS) mode to obtain the specific imaging, i.e. the characteristic NEXAFS of the polymers was employed to ascertain the component lateral distribution. A distinction between the polymers is possible because the sharp peak at 285.2 eV in the NEXAFS spectrum of PS, corresponding to the C = C π to π* transition of the aromatic group, is not visible in the spectrum of PBMA(Fig. 1). High absorption of synchrotron radiation corresponding to core levels result in a high yield of secondary electrons by the amplification of the Auger electrons produced. The sample image intensity (I_{max}) recorded in an acquisition time of 8 min with a 70-μm contrast aperture at the maximum of the absorption edge at 285.2 eV was digitally compared, pixel by pixel, with the image intensity (I_{back}) taken at 284 eV on the background below the edge. In the resulting difference image, $I_{diff} = I_{max} - I_{back}$, the bright features thus represent the PS-rich phase. An approximate length scale could be provided by comparing the PEEM micrograph with an image of the same sample taken with an optical microscope.

Secondary ion mass spectroscopy
The equipment and conditions for analysis have been described previously [3]. The pure components gave SIMS spectra similar to literature data and inspection showed that the polymers could be distinguished by their characteristic fragments, for example, $C_7D_7^+$ for the poly(dg-styrene). Quantification generally requires the relative SIMS sensitivities of the blend components but, as will be seen later, in this case only one component was detected at the film surface by SIMS.

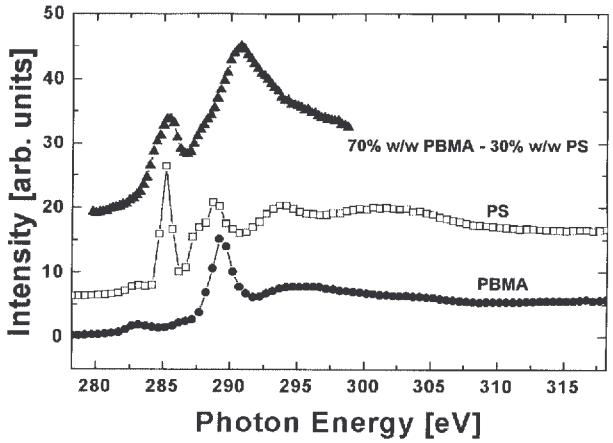

Fig. 1 Near-edge X-ray absorption fine structure spectra of the carbon K edge of polystyrene (PS), poly(n-butyl methacrylate) (PBMA) and a blend containing 70% w/w PBMA. The spectra are not plotted to scale

X-ray photoelectron spectroscopy
The equipment and conditions for analysis have also been described previously [3]. PS exhibits a single Cl*s* peak at a binding energy of 284.6 eV, corresponding to carbon joined only to carbon, with a *π-π**

satellite [11] at about 7 eV higher binding energy, which is of low intensity and falls outside the Cl*s* envelope of PBMA.

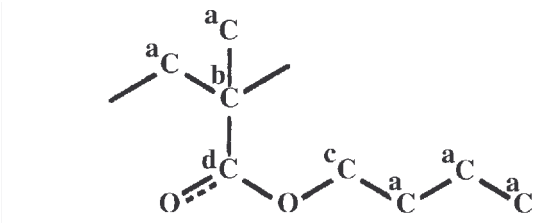

The latter has three electron deficient carbon environments b-d, with binding energy shifts relative to ^{a}C of 0.7, 1.7 and 3.9 eV, respectively [12], and relative intensities $I(^{b}C) = I(^{c}C) = I(^{d}C) = I(^{a}C)/5$. The Cl*s* envelope for pure PBMA with the individual spectral contributions is shown in Fig. 2. The carboxyl carbon, ^{d}C, can be readily distinguished and was used, therefore, for quantification. The Cl*s* envelope for a blend will contain the PBMA contributions plus the PS contribution, which is coincident with ^{a}C. Accordingly, the Cl*s* envelope for a blend was reconstructed by peak synthesis, first obtaining the carboxyl contribution then assuming the above binding energies and relative intensities to obtain the total Cl*s* contribution from PBMA. The remaining signal at 284.6 eV was taken as the total Cl*s* contribution from PS. Both monomers have eight carbon atoms; thus, the relative monomer concentrations are equal to the relative Cl*s* contributions.

Results

Atomic force microscopy
AFM images of PS—PBMA blends over a range of compositions are shown in Fig. 3. The films are relatively smooth until the PBMA content is above 50% w/w. Over the range 60-70% w/w PBMA ribbonlike structures are observed and for PBMA contents above 70% w/w discrete islands are formed, which decrease in diameter with an increase in PBMA concentration.

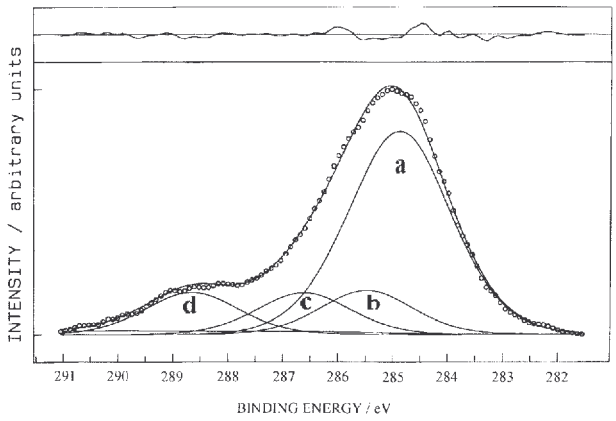

Fig. 2 X-ray photoelectron spectroscopy (XPS) Cls spectrum of pure PBMA. The spectrum is deconvoluted to show the contributions from the various carbon species

Published in: Colloid polymer science (2000), vol. 278, iss. 10, pp. 993-999
Status: Postprint (Author's version)

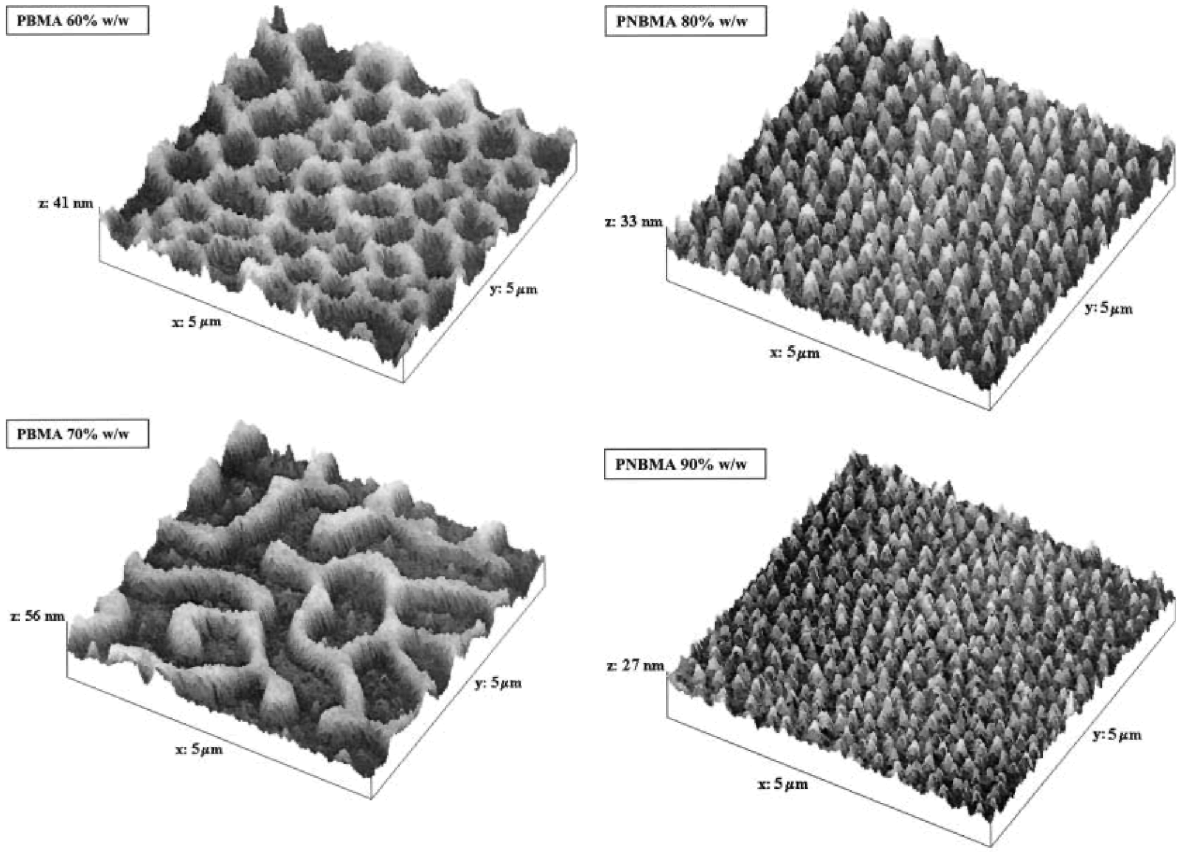

Fig. 3 Atomic force microscopy (AFM) images of various compositions of PS-PBMA blends. The area shown is always the same, while the height scale varies according to the range of surface structure

The pixel height distributions for each image are shown in Fig. 4. The ribbonlike structures, PBMA 60 and 70% w/w, have a major peak corresponding to the valley level, plus a distinct peak corresponding to the raised component. The latter contribution reduces to a shoulder for the island-type structures, PBMA 80 and 90% w/w. The relative area corresponding to the raised component obviously decreases with a decrease in the PS content. The area occupied by the raised features was estimated by subtracting the valley contribution, fitted with a Gaussian profile, from the total area. The results show a close correlation with the PS content (Table 2).
A "characteristic height" for the topographical features was obtained by fitting a second peak, which was slightly asymmetric to lower heights, and measuring the distance between peak maxima. Though not completely unambiguous, the relative positions of the maxima provide a useful measure of the differential height. The dimensions of the features are noted in Table 2. Whilst the film thickness is approximately constant at 43 ± 4 nm over the full range of compositions, the ribbon structure at PBMA 70% w/w forms the most prominent topography. In the region of island formation, the relative height of the islands is approximately constant, but their diameter decreases with a decrease in the PS content.

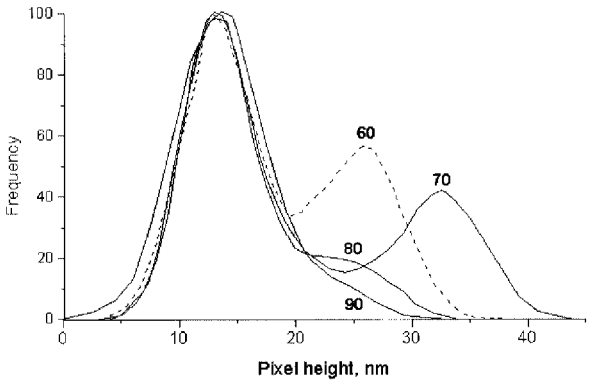

Fig. 4 AFM pixel height distributions for various blends. The labels on the curves indicate the PBMA

content

Table 2 Film dimensions

% w/w polystyrene	Film thickness (nm)	Film features	% area polystyrene	Feature height (nm)	Feature diameter (nm)
90	42 ± 2	None	_	_	_
70	46 ± 3	None	-	-	-
50	39 ± 3	None	-	-	-
40	43 ± 3	Ribbons	41	13 ± 0.5	-
30	46 ± 2	Ribbons	31	18 ± 0.5	-
20	44 ± 2	Islands	23	11 ±0.5	323 ± 42
10	45 ± 3	Islands	10	11 ±0.5	195 ± 27

XPS and SIMS

The surface versus the bulk compositions of the blends are given in Fig. 5. The SIMS data show that only PBMA is present in the topmost surface over the full composition range. The XPS data show an increasing concentration of PBMA up to 50% w/w bulk concentration, at which point the surface is mainly covered with the polyester and the XPS and SIMS data start to converge. SIMS and XPS probe to depths of about 0.5-1.0 and 5 nm, respectively; thus, there is a concentration gradient within the first 5-nm depth for compositions below 50% w/w PBMA. At higher PBMA contents the composition of the surface region approaches saturation with PBMA.

Photoemission electron microscopy

The PS-selective image of the 96-nm thick film of the PS-PBMA blend with a PBMA content of 70% w/w is shown in Fig. 6. It reveals that there are ribbons of high intensity (displayed on a height scale) corresponding to a PS-rich phase, in a low intensity sea corresponding to a PBMA-rich phase. At a PBMA content of 70% w/w the XPS data showed that the surface of the 43-nm thick film was mainly covered by PBMA to a depth of about 5 nm or more, whereas the PEEM data showed a marked amount of PS. The differences between the XPS and PEEM data arise from differences in the techniques and the samples. Even with a small signal from PS, PEEM can distinguish the lateral segregation of the components because it is sensitive to the contrast along the surface, whereas separating out a small PS component from the PS/PBMA C1*s* envelope in the XPS data is subject to the error of measuring the minor carboxyl signal. Also, it is probable that the slightly different casting conditions and lower-molecular-weight PBMA used in the PEEM study resulted in a real lowering of the segregation of the PBMA to the surface, making the overlayer thinner and the PS more evident with PEEM.

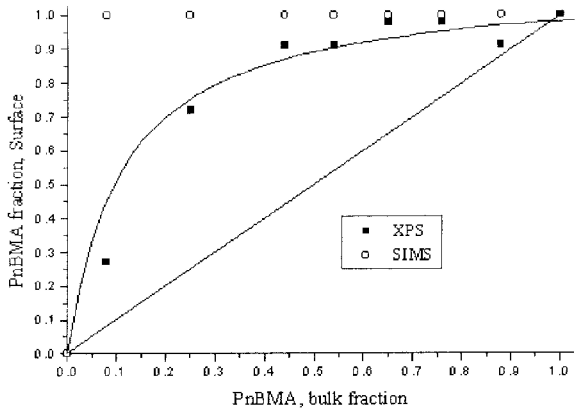

Fig. 5 Surface concentration of PBMA from XPS and secondary ion mass spectroscopy (SIMS) as a function of the bulk concentration for blend films. The penetration depths of the techniques are about 5 and 1 nm, respectively; therefore, SIMS provides the concentration at the outermost surface, whilst XPS gives the near-surface composition. The straight line assumes the surface is the same as the bulk. The errors are approximately 10%

Published in: Colloid polymer science (2000), vol. 278, iss. 10, pp. 993-999
Status: Postprint (Author's version)

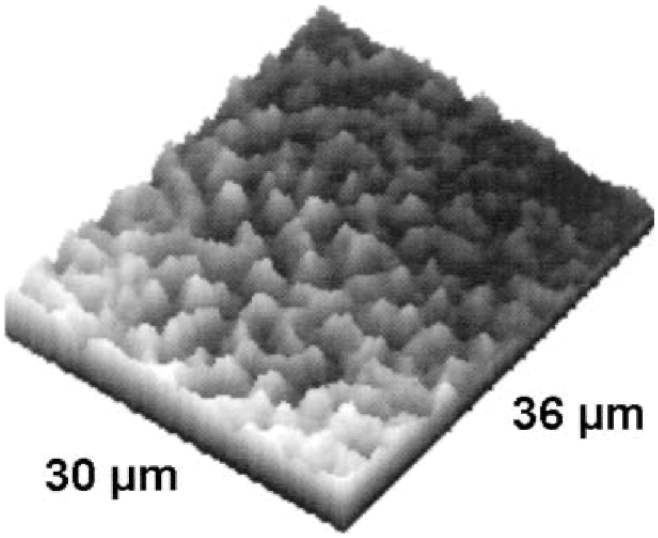

Fig. 6 Photoemission electron microscopy PS-selective spectrum of a 96-nm thick PS-PBMA blend with a PBMA content of 70% w/w. The intensity is plotted on a height scale; thus, PS-rich regions appear as raised features

The only conclusion that is taken from the comparison of the XPS/AFM and PEEM data is that similar structures are observed with the same blend system using different techniques, i.e. the model of a film with elevated features of a PS-rich phase is confirmed.

Discussion

It is convenient to discuss the behaviour of PS-poly(alkyl acrylate) blends using the model provided by the PS-PBr_xS system. The factors which control the thin film structure are the polymer compatibilities, the surface free energies, the nature of the substrate and the solvent used for casting. With the highly incompatible $PBr_{1.0}S$-dPS system [3], the phases separate to give almost pure components and the more polar component forms elevated regions. SIMS showed that the surface contained both components, but there was a slight excess of the dPS.
Both Tanaka et al. [7] and Walheim et al. [9] found that for the highly incompatible PS—PMMA system, films cast from toluene on Si(O) phase-separate to form elevated islands/ribbons of PMMA. The marked chemical difference between PMMA and PS leads to a significant difference in solubility behaviour between the components, and Walheim et al. [9] showed that the component which is raised can be altered by control of the solvent. For PS-PMMA films cast from toluene, film formation is via a precursor in which the PS is preferentially swollen. Even films of PS-PMMA several microns thick, cast from toluene onto quartz, can have rough surfaces with the polyester protruding [13]. PMMA has a higher surface energy than PS and only segregates to the surface if its relative M_n is low [8]; thus, the surface consists of areas of PMMA and PS. Tanaka et al. [7] conclude that the PMMA phase in an approximately symmetric blend contains a small amount of PS, which goes to the polymer-air surface and lowers the surface tension, thus favouring the relative increase in area of the PMMA-rich phase. When the polymers in the blend become more compatible phase separation is less probable. Again, the PS-PBr_xS system provides the model. Decreasing the bromine content makes PBrS more compatible with PS and the topography of thin films of a $PBr_{0.33}S$—dPS blend is less marked than with the fully brominated polymer and occurs only over a restricted composition range [6]. In addition, in the composition region where the film is smooth there is segregation to the polymer-air interface, the surface of the unannealed film being completely covered by dPS. A picture emerges from the PBr_xS-dPS study [6] of the blend forming a single phase at low polymer incompatibilities then, as the incompatibility is increased, the lower-surface-energy component increasingly segregates to the air interface. Eventually, the incompatibility is sufficient to induce phase separation. When the incompatibility is increased further the phase separation becomes more pronounced, producing nearly pure components at the surface and the segregation at the polymer—air interface decreases.
Neutron reflectivity studies of the interfacial width of PS-PMMA bilayers give values of 5 nm at 170°C, i.e. the blend is highly incompatible, whereas PS-PBMA bilayers are more compatible, with an

interface width of about 9 nm at 156 °C [14]. Nevertheless, the incompatibility of blends of the latter system containing more than 50% w/w PBMA is sufficient to produce phase separation in thin cast films. When topography is observed on the thin films of dPS-PBMA the XPS data show that most of the surface is covered by an overlayer of PBMA reaching at least 5-nm thickness. On the other hand, the correlation of the relative area of the features with the dPS concentration suggests that the elevated features are composed mainly of dPS. Together, the data are consistent with a film structure formed from droplets of dPS dispersed in a PBMA matrix, similar to thin films of PS—poly(vinylmethylether), in which the surface is completely covered by the low-surface-energy component [4].

PS-PMMA films are rough even at PMMA contents of about 2% w/w [8]. When the PBMA content decreases to 50% w/w or less in the PS-PBMA blends the films are relatively smooth. SIMS shows that the surface is always covered by a very thin film of PBMA, whilst XPS shows that the near surface becomes more saturated with PBMA as the concentration increases from 0 to 50% w/w. The surface analyses suggest that at low PBMA concentrations the PBMA molecule is spread over the surface, thereby reducing the surface energy. As the concentration increases the PBMA molecules can pack the surface without adopting an energetically unfavourable extended configuration, thus the PBMA overlayer thickness increases. If the overlayer at high PBMA concentrations consisted of a complete monolayer of coiled molecules, the XPS PS signal would not be detectible because the XPS probe depth is less than R_g. The small XPS signal observed from PS at high PBMA concentrations suggests that the overlayer is not uniform or that there is some interdiffusion of the PS and PBMA chains.

The buildup of PBMA at the polymer—air interface, and a similar effect occurring at the hydrophilic substrate surface, will decrease the PBMA concentration in the remainder of the film. PS-PBMA blends are only moderately incompatible, according to the measurement of interfacial width of the corresponding bilayer, and segregation will produce a marked lowering of the PBMA concentration in the interior of the film, which is only 43-nm thick overall. Hence, at low PBMA contents the consequence of increased compatibility and lower surface energy, compared to PS-PMMA, would be to move the system effectively into the one-phase region, producing a smooth surface.

Conclusions

The variety of surface analysis techniques used, AFM, XPS, SIMS and PEEM, provided information on different aspects of the structure of the spin-cast films of the weakly incompatible polymers; thus, information was obtained on surface segregation and lateral phase separation. Films with PBMA contents lower than 50% w/w were relatively smooth, but protruding ribbons or islands of constant height were observed at medium and high PBMA contents. Estimates from the AFM topographs of the area occupied by the raised features showed that it correlated with the PS content. Additional evidence for the features being a PS-rich phase was given by the PEEM study. The PS-selective PEEM image showed PS-rich ribbon structures, similar to the ribbon features observed with AFM, for films with the same blend composition of 70% w/w PBMA. SIMS showed that at all blend compositions the topmost surface was covered by PBMA, whereas the concentration of PBMA in the near-surface region was shown by XPS to increase with bulk concentration, eventually to near saturation.

In contrast to PS-PMMA blends, in PS-PBMA mixtures the lower surface energy of the butyl ester causes interfacial segregation and therefore depletion of PBMA in the "bulk" of the thin film. Combined with the greater polymer compatibility of PS-PBMA, compared to PS-PMMA, the effective composition in the "bulk" is moved into the single-phase region when the overall PBMA content is less than 50% w/w. Thus, thin films with PBMA contents below 50% w/w are smooth and films with PBMA contents above 50% w/w have topography.

Acknowledgements
We are grateful to Th. Wagner for help with sample preparation and characterisation and to O. Schmidt, in the group of G. Schonhense of Mainz University, for assistance with the PEEM experiments. We also appreciate financial support from the EPSRC (studentship), the BMBF (project F13MPG) and the EU (framework contracts CT930351 and CT930370).

References

[1] Bruder F, Brenn R (1992) Phys Rev Lett 69:624
[2] Tanaka K, Yoon J-S, Takahara A, Kajiyama T (1995) Macromolecules 28:934
[3] Affrossman S, Henn G, O'Neill SA, Pethrick RA, Stamm M (1996) Macro-molecules 29:5010

[4] Ermi BD, Karim A, Douglas JF (1998) J Polym Sci Part B Polym Phys 36:191
[5] Guckenbiehl B, Stamm M, Springer T (1994) Physica B 198:127
[6] Affrossman S, O'Neill SA, Stamm M (1998) Macromolecules 31:6280
[7] Tanaka K, Takahara A, Kajiyama T (1996) Macromolecules 29:3232
[8] Tanaka K, Takahara A, Kajiyama T (1998) Macromolecules 31:863
[9] Walheim S, Böltau M, Mlynek J, Krausch G, Steiner U (1997) Macromolecules 30:4995
[10] Swiech W, Fecher GH, Ziethen Ch, Schmidt O, Schonhense G, Grzelakow-ski K, Schneider CM, Fromter R, Oepen HP, Kirschner J (1997) J Electron Spectrosc Relat Phenom 84:171
[11] Clark DT, Adams DB, Dilks A, Peeling J, Thomas HR (1976) J Electron Spectrosc Relat Phenom 8:51
[12] Briggs D, Beamson G (1992) Anal Chem 64:1729
[13] Kumacheva E, Li L, Winnik MA, Shinozaki DM, Cheng PC (1997) Langmuir 13:2483
[14] Stamm M, Schubert DW (1995) Annu Rev Mater Sci 25:325